

Cation-Controlled Photophysics in a Re(I) Fluoroionophore

D. Brent MacQueen and Kirk S. Schanze*

Contribution from the Department of Chemistry, University of Florida,
Gainesville, Florida 32611. Received February 21, 1991

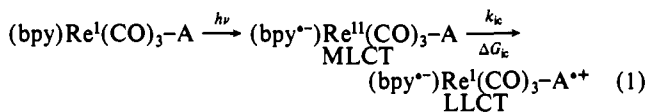
Abstract: Alkali and alkaline earth metal cations have a profound effect on the photophysics of the $d\pi(\text{Re}) \rightarrow \pi^*$ (bpy) metal-to-ligand charge-transfer (MLCT) excited state in crown ether substituted complex **1**. The unique cation-induced effects arise because of the influence of the "crowned" cation on the energy of the ligand-to-ligand charge-transfer (LLCT) excited state that is formed by charge transfer from the donor nitrogen to the electron-deficient metal center in the MLCT state



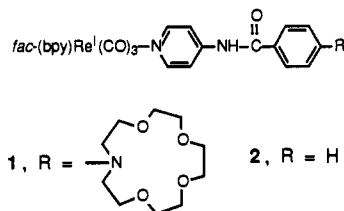
(where bpy = 2,2'-bipyridine and A = the amine donor). In the absence of cations, the energy of the LLCT state lies below the MLCT state. As a result, k_{ic} is large and the LLCT state provides a path for rapid radiationless decay of the MLCT state. However, due to the ion-dipole interaction between the cation and the donor nitrogen in cation-crown complexes ($1 \cdots M^{\text{II}}$), the energy of the LLCT state is higher than that of the MLCT state. Under these conditions, the MLCT state decays primarily by "normal" radiative and nonradiative decay paths. As a result, the MLCT emission yield is larger for the $1 \cdots M^{\text{II}}$ complexes compared to that for **1**. Emission quantum yield and lifetime data for the $1 \cdots M^{\text{II}}$ complexes are interpreted by a kinetic model in which the rate-determining step for excited-state decay involves dissociation of the cation from the macrocycle. The crown-substituted complex **1** provides a paradigm for a MLCT-based cation sensor.

Introduction

In complexes of the type *fac*-(bpy)Re^I(CO)₃-A (where bpy is 2,2'-bipyridine and A is an aromatic amine), the $d\pi(\text{Re}) \rightarrow \pi^*$ (bpy) metal-to-ligand charge-transfer (MLCT) excited state is strongly quenched via intramolecular aniline to Re charge transfer.¹ This process results in formation of a ligand-to-ligand charge-transfer (LLCT) excited state:



Since the MLCT state is luminescent²⁻⁵ and the LLCT state is not,¹ it occurred to us that if the rate of internal conversion (k_{ic}) could be decreased by addition of alkali or alkaline earth metal ions, then a (bpy)Re^I(CO)₃-A complex could provide the basis for a luminescent cation sensor. Recent studies of chromophore and redox-site substituted ionophores suggested that incorporation of the donor amino group into the crown macrocycle in complex **1** would make it possible to achieve this goal.⁶⁻¹²



(1) (a) Schanze, K. S.; Cabana, L. A. *J. Phys. Chem.* **1990**, *94*, 2740. (b) Perkins, T. A.; Humer, W.; Netzel, T. L.; Schanze, K. S. *J. Phys. Chem.* **1990**, *94*, 2229. (c) MacQueen, D. B.; Perkins, T. A.; Schmehl, R. H.; Schanze, K. S. *Mol. Cryst. Liq. Cryst.* **1991**, *194*, 113.

(2) Wrighton, M.; Morse, D. L. *J. Am. Chem. Soc.* **1974**, *96*, 998.

(3) Caspar, J. V. Ph.D. Dissertation, University of North Carolina at Chapel Hill, 1982.

(4) Juris, A.; Campagna, S.; Bidd, I.; Lehn, J.-M.; Ziessel, R. *Inorg. Chem.* **1988**, *27*, 4007.

(5) Sacksteder, L.; Zipp, A. P.; Brown, E. A.; Streich, J.; Demas, J. N.; DeGraff, B. A. *J. Phys. Chem.* **1990**, *29*, 4335.

(6) For an excellent review, see: Lohr, H.-G.; Vogtle, F. *Acc. Chem. Res.* **1985**, *18*, 65.

(7) Sousa, L. R.; Larson, J. M. *J. Am. Chem. Soc.* **1977**, *99*, 307.

(8) Jonker, S. A.; Ariese, F.; Verhoeven, J. W. *Recl. Trav. Chim. Pays-Bas* **1989**, *108*, 109.

(9) Bourson, J.; Valeur, B. *J. Phys. Chem.* **1989**, *93*, 3871.

(10) Echegoyen, L. E.; Yoo, H. K.; Gatto, V. J.; Gokel, G. W.; Echegoyen, L. *J. Am. Chem. Soc.* **1989**, *111*, 2440.

The present paper presents the results of photophysical and electrochemical studies of **1**. Photophysical data suggest that exceedingly rapid internal conversion occurs in the free complex, and as a result, only weak MLCT emission is observed. However, the quantum yield and lifetime (Φ_{em} and τ_{em} , respectively) of the MLCT emission increase substantially by addition of alkali and alkaline earth metals. This work provides the first example of a compound in which the photophysical properties of an MLCT chromophore can be strongly influenced by metal cations. In addition, luminescence decay kinetics of alkali and alkaline earth metal complexes of **1** suggest that the decay rate of the MLCT state is controlled, in part, by the rate of dissociation of the cation from the crown macrocycle. This indicates that luminescence decay studies of **1** and related complexes may provide a direct method for determining dissociation rates for cation-crown complexes.

Experimental Section

Preparations. *N*-Benzoyl-4-aminopyridine. 4-Aminopyridine (5.0 g, 53 mmol) and triethylamine (10.7 g, 100 mmol) were mixed in 50 mL of CH_2Cl_2 . Benzoyl chloride (7.5 g, 100 mmol) was added slowly with stirring to the CH_2Cl_2 solution. (This reaction is highly exothermic.) After cooling, the reaction mixture was extracted with aqueous Na_2CO_3 , the organic phase was dried over Na_2SO_4 , and then the solvent was evaporated. The crude product was purified by recrystallization from $\text{EtOH}/\text{H}_2\text{O}$. The product was obtained as white needles: yield 5.0 g (51%); ¹H NMR (300 MHz, CDCl_3) δ 7.50-7.65 (m, 5 H, benzoyl), 7.88 (d, 2 H, pyridyl), 8.04 (br s, 1 H, NH), 8.56 (d, 2 H, pyridyl).

4-(4,7,10,13-Tetraoxa-1-azacyclopentadecyl)benzoic Acid. 4-(4,7,10,13-Tetraoxa-1-azacyclopentadecyl)benzaldehyde¹³ (5.0 g, 15 mmol) and anhydrous MgSO_4 (1.9 g, 15 mmol) were mixed with 100 mL of acetone in a three-necked flask equipped with an addition funnel, a reflux condenser, and a stirbar. A solution of KMnO_4 (3.6 g, 23 mmol) dissolved in 100 mL of acetone was added via the addition funnel to the stirred solution of the benzaldehyde over the course of 90 min, and the resulting solution was stirred at 25 °C for 60 min. Then the acetone was removed by rotovap, and the product was dissolved in 100 mL of hot H_2O . The aqueous solution was washed with 50 mL of CH_2Cl_2 and then acidified to pH 4 by addition of 1 M HCl. Upon acidification, a solid precipitates, which was collected by filtration. The aqueous filtrate was then extracted two times with 50-mL portions of CH_2Cl_2 . The CH_2Cl_2 fraction was dried (Na_2SO_4), and the solvent was evaporated. The residue, combined with the solid that precipitated after acidification, was

(11) Beer, P. D.; Blackburn, C.; McAleer, J. F.; Sikanyika, H. *Inorg. Chem.* **1990**, *29*, 378.

(12) Fages, F.; Desvergne, J.-P.; Bouas-Laurent, H.; Marsau, P.; Lehn, J.-M.; Kotzyba-Hilbert, F.; Albrecht-Gary, A.-M.; Al-Joubbeh, M. *J. Am. Chem. Soc.* **1989**, *111*, 8672.

(13) Dix, J. P.; Vogtle, F. *Chem. Ber.* **1980**, *113*, 457.

dissolved in 100 mL of CH_2Cl_2 , and the solution was washed three times with H_2O to remove any ions that might be complexed by the crown. The CH_2Cl_2 solution was dried (Na_2SO_4), and the solvent was evaporated. The crude product was purified by chromatography (silica gel, 200–400 mesh, 5% $\text{MeOH}/\text{CH}_2\text{Cl}_2$ eluant). The carboxylic acid was identified on the column by its characteristic green emission. The product was collected as a pale yellow solid: yield 1.5 g (30%); $^1\text{H NMR}$ (300 MHz, CDCl_3) δ 3.6–3.8 (m, 20 H, aliphatic crown), 6.65 (d, 2 H, aromatic), 7.85 (d, 2 H, aromatic).

N-[4-(4,7,10,13-Tetraoxa-1-azacyclopentadecyl)benzoyl]-4-aminopyridine. The azacrown-substituted benzoic acid (630 mg, 1.9 mmol) was combined with SOCl_2 (325 mg, 2.7 mmol) and DMF (0.15 mL, 1.9 mmol) in 20 mL of toluene.¹⁴ The solution was heated to 70 °C for 1 h, and then the solvent was removed by rotovap. The resulting acid chloride was dissolved in 20 mL of CH_2Cl_2 , and then triethylamine (1.5 mL, 11 mmol) and 4-aminopyridine (175 mg, 1.9 mmol) were added. The resulting solution was stirred at 25 °C overnight. The reaction mixture was extracted with aqueous Na_2CO_3 , the organic phase was dried over Na_2SO_4 , and then the solvent was evaporated. The crude product was purified by chromatography (silica gel, 200–400 mesh, 5% $\text{MeOH}/\text{CH}_2\text{Cl}_2$ eluant). The amide was obtained as a pale yellow solid: yield 320 mg (43%); $^1\text{H NMR}$ (300 MHz, CDCl_3) δ 3.6–3.8 (m, 20 H, aliphatic crown), 6.6 (d, 2 H, aromatic), 7.7 (d, 2 H, pyridyl), 7.8 (d, 2 H, aromatic), 8.45 (d, 2 H, pyridyl), 8.8 (s, 1 H, N H); high-resolution mass spectrum, m/z (relative intensity, %) 415.2104 (M^+ , $\text{C}_{22}\text{H}_{29}\text{N}_3\text{O}_5$, 100) (calcd 415.2108), 322 (80), 294 (16), 292 (17), 234 (15), 204 (30), 146 (18), 132 (18).

Metal Complex 1. The azacrown-substituted pyridine (100 mg, 0.24 mmol) and [(2,2'-bipyridyl) $\text{Re}^{\text{I}}(\text{CO})_3(\text{triflate})$]¹⁵ (154 mg, 0.27 mmol) were dissolved in 20 mL of THF, and the solution was gently refluxed under Ar overnight. After cooling, the THF was removed by rotovap and the residue was dissolved in 20 mL of acetone/ H_2O (1:1 v/v). The complex was precipitated by addition of a concentrated aqueous NH_4PF_6 solution. The precipitate was collected by filtration, dried, and then reprecipitated by dissolving in a minimum volume of acetone and dropping into diethyl ether. The product was obtained as a pale yellow powder: yield 125 mg (53%). Final purification was effected by repeated chromatography (silica gel, 200–400 mesh, 5% $\text{MeOH}/\text{CH}_2\text{Cl}_2$ eluant): $^1\text{H NMR}$ (300 MHz, CDCl_3) δ 3.5–3.8 (m, 20 H, aliphatic crown), 6.55 (d, 2 H, benzoyl), 7.65 (m, 4 H, pyridyl and benzoyl), 7.75 (t, 2 H, bpy), 7.85 (d, 2 H, pyridyl), 8.20 (t, 2 H, bpy), 8.40 (d, 2 H, bpy), 8.9 (s, 1 H, NH), 9.1 (d, 2 H, bpy). Anal. Calcd for $\text{C}_{35}\text{H}_{37}\text{N}_3\text{O}_8\text{RePF}_6$: C, 42.60; H, 3.78; N, 7.10. Found: C, 41.02; H, 3.53; N, 6.75.

Metal Complex 2. The complex was prepared as described for 1 except that *N*-benzoyl-4-aminopyridine was used in place of the azacrown-substituted pyridine: yield 110 mg (60%); $^1\text{H NMR}$ (300 MHz, acetone- d_6) δ 7.48 (t, 2 H, phenyl), 7.60 (m, 1 H, phenyl), 7.82 (d, 2 H, pyridyl), 7.91 (d, 2 H, phenyl), 8.00 (t, 2 H, bpy), 8.37 (d, 2 H, pyridyl), 8.47 (t, 2 H, bpy), 8.73 (d, 2 H, bpy), 9.47 (d, 2 H, bpy), 10.20 (s, 1 H, NH). Anal. Calcd for $\text{C}_{25}\text{H}_{18}\text{N}_4\text{O}_8\text{RePF}_6$: C, 39.02; H, 2.36; N, 7.28. Found: C, 39.05; H, 2.40; N, 7.06.

Equipment. Steady-state luminescence spectra were obtained on a Spex Industries F-112A spectrophotometer. Emission spectra were corrected for instrument response with correction factors generated by using a tungsten filament primary standard lamp. Excitation spectra were corrected by using a Rhodamine B/1,2-propanediol quantum counter reference. Emission lifetimes were determined by time-correlated single-photon counting on a commercially available instrument (Photochemical Research Associates).¹⁶ The excitation source was a H_2 -filled spark gap, and the instrument response was ~ 2.0 ns fwhm. Excitation light was filtered with a near-UV band-pass filter (Schott, UG-11, maximum transmittance at 350 nm), and emission light was filtered with a 70-nm band-pass interference filter (maximum transmittance at 550 nm). The luminescence decays were analyzed by using a computer program that deconvolutes the instrument response from the sample emission profile. UV-visible spectra were recorded on a Perkin-Elmer Model 320 spectrophotometer. Cyclic voltammetry was carried out at a Pt working electrode (with Pt auxiliary and SSE reference electrodes) by using a Bioanalytical Systems CV-2 voltammograph.

UV-Visible and Luminescence Experiments. In order to achieve reproducible equilibrium constants for binding of cations to 1, it was necessary to ensure that all materials and solvents were anhydrous. Complex 1, the metal perchlorate salts, and tetrabutylammonium perchlorate

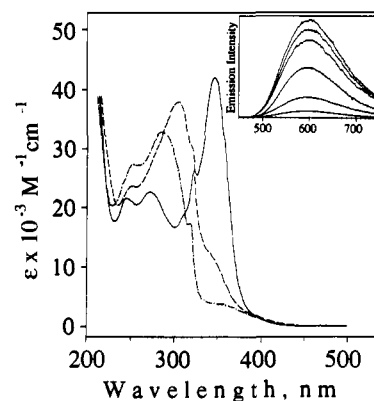


Figure 1. UV-visible absorption spectra of Re(I) complexes in CH_3CN solution: (—) 1; (---) 1 + 0.1 M Ca^{2+} ; (-·-·-) 2. The inset is emission spectra of 1 in CH_3CN solution, scaled according to relative emission quantum yield ($\lambda_{\text{ex}} = 320$ nm, which is the isosbestic point in the Ca^{2+} titration). In order of increasing emission intensity, $[\text{Ca}^{2+}] = 0, 0.001, 0.002, 0.003, 0.004,$ and 0.005 M.

Table I. Association Constants and Photophysical Properties for Re(I) Complexes^a

complex	K_a^b	$\Phi_{\text{em}}^{\text{max}c}$	$\tau_{\text{em}}, \text{ns}^d$	$k_r, \text{s}^{-1}e$
1		0.0017	<1	<i>f</i>
1... Na^+	140	0.0049	7.3	6.7×10^5
1... Ba^{2+}	560	0.0066	32	2.1×10^5
1... Ca^{2+}	3900	0.012	60	2.2×10^5
1... H^+		0.025	159	1.6×10^5
2		0.020	147	1.4×10^5

^a All data in CH_3CN solution. ^b Association constants. ^c Maximum emission quantum yield (see text) for Ar-purged solution; estimated error $\pm 20\%$. Actinometer: $\text{Ru}(\text{bpy})_3^{2+}$ in degassed H_2O , $\Phi_{\text{em}} = 0.042$ (ref 18). A correction was applied because of the difference in refractive index of CH_3CN and H_2O . ^d Emission lifetime of Ar-purged solution ($\lambda_{\text{ex}} = 350$ nm, $\lambda_{\text{em}} = 550$ nm); estimated error $\pm 5\%$. ^e Radiative rate constant, calculated from ratio $\Phi_{\text{em}}/\tau_{\text{em}}$. ^f Emission too weak for reliable estimate.

(TBAP) were dried in a vacuum oven at 60 °C overnight, and CH_3CN was dried by distillation from P_2O_5 . All experiments were conducted in CH_3CN with 0.1 M TBAP added to maintain constant ionic strength (or as a supporting electrolyte). UV-visible, steady-state, and time-resolved emission titrations were carried out by placing a 3-mL aliquot of a solution containing 1 ($c \approx 2 \times 10^{-5}$ M) in a quartz cuvette fitted with a septum cap, outgassing with Ar, and then recording spectra after each addition of a 5- μL aliquot of a concentrated (e.g., 1.0 M) metal perchlorate solution in CH_3CN . Association constants were determined from the UV-visible titrations by a literature method.^{8,17} When relative emission intensities were determined as a function of [cation], the excitation wavelength corresponded with the isosbestic point in the absorption spectrum. Emission quantum yields and lifetimes for the 1... M^+ complexes were determined by using solutions of 1 + 0.1 M cation; emission titration studies confirmed that [cation] = 0.1 M was sufficient to ensure that 1 was fully complexed. The effect of protonation on the photophysical properties of 1 was examined by addition of concentrated HClO_4 (70%) to a CH_3CN solution of 1 ($[\text{H}^+] \approx 0.05$ M). Emission quantum yields were determined relative to $\text{Ru}(\text{bpy})_3^{2+}$ in Ar-outgassed H_2O ($\Phi_{\text{em}} = 0.042$).¹⁸

Results and Discussion

Complex 2 serves as a model for the photophysical properties of the $d\pi(\text{Re}) \rightarrow \pi^*(\text{bpy})$ MLCT excited state. The absorption spectrum of 2 (Figure 1) displays weak MLCT absorption at 350 nm ($\epsilon = 4.1 \times 10^3 \text{ M}^{-1} \text{ cm}^{-1}$), and more intense π, π^* intraligand absorptions at shorter wavelength. The complex also exhibits moderately intense MLCT emission with $\lambda_{\text{max}} = 597$ nm; relevant photophysical parameters are listed in Table I.

The absorption spectrum of 1 (Figure 1) is similar to the spectrum of the model, except for a strong band at $\lambda_{\text{max}} = 340$

(14) Munakata, K.-I.; Tanaka, S.; Toyoshima, S. *Chem. Pharm. Bull.* **1980**, *28*, 2045.

(15) Caspar, J. V.; Sullivan, B. P.; Meyer, T. J. *Organometallics* **1983**, *2*, 551.

(16) O'Connor, D. V.; Phillips, D. *Time-Correlated Single Photon Counting*; Academic: New York, 1984.

(17) Foster, R. *Organic Charge-Transfer Complexes*; Academic: New York, 1969.

(18) Van Houten, J.; Watts, R. J. *J. Am. Chem. Soc.* **1976**, *98*, 4853.

nm ($\epsilon \approx 4.2 \times 10^4 \text{ M}^{-1} \text{ cm}^{-1}$). This band is assigned to an intraligand charge-transfer (ILCT) transition of the azacrown-substituted *N*-benzoyl-4-aminopyridine ligand in which the crown nitrogen serves as a donor atom.¹⁹ The Re \rightarrow bpy MLCT absorption appears as a tail on the ILCT band. However, in contrast to the model, **1** exhibits only weak MLCT emission (compare Φ_{em} and τ_{em} for **1** and **2**, Table I). The MLCT quenching in **1** is attributed to rapid internal conversion to an energetically low lying LLCT state (k_{ic} , eq 1).

Electrochemical and spectroscopic data indicate that internal conversion in **1** is exoergic ($\Delta G_{\text{ic}} < 0$). Cyclic voltammetry of **1** reveals reversible cathodic ($E_{1/2} = -1.18 \text{ V}$) and anodic ($E_{1/2} = +1.11 \text{ V}$) waves, which are assigned to reduction of the bipyridine ligand (bpy/bpy $^{\cdot-}$) and to oxidation of the azacrown donor ligand (A/A $^{+}$), respectively.¹ By using these potentials along with the energy of the MLCT state (2.43 eV, determined from the emission spectrum of the complex), ΔG_{ic} is estimated to be -0.14 eV .²⁰

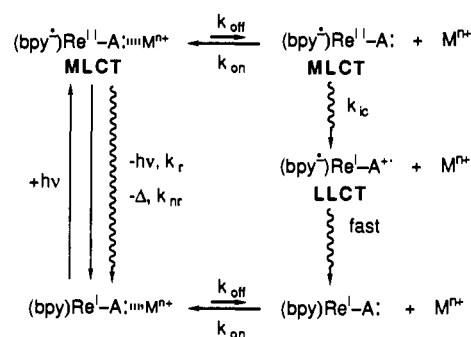
Alkali and alkaline earth metal cations have profound effects on the photophysical and electrochemical response of **1**. Addition of Na $^+$, Ba $^{2+}$, or Ca $^{2+}$ leads to dramatic changes in the near-UV absorption. For example, Figure 1 compares the spectra of **1** and **1** + 0.1 M Ca $^{2+}$; complexation of Ca $^{2+}$ decreases the donor ability of the crown nitrogen, which leads to a significant blue shift of the ILCT absorption. Similar, but less dramatic shifts are observed upon coordination of Na $^+$ and Ba $^{2+}$ to **1**. Equilibrium association constants, determined by UV-visible titration of **1** with metal cations (K_a , Table I),^{8,17} increase along the series Na $^+$ < Ba $^{2+}$ < Ca $^{2+}$, and their absolute values are very similar to those observed in studies of other aza-15-crown-5 ionophores.²¹

Addition of metal cations to **1** leads to a significant increase in the MLCT emission yield (Φ_{em}). For example, Figure 1 (inset) illustrates the increase in Φ_{em} that occurs upon addition of Ca $^{2+}$; similar but attenuated effects occur upon addition of Na $^+$ and Ba $^{2+}$. The titration curves (Φ_{em} vs [M $^{n+}$]) for each cation are quantitatively consistent with the equilibrium, **1** + M $^{n+}$ \rightarrow **1**...M $^{n+}$, where **1**...M $^{n+}$ is more strongly luminescent than **1**. Maximum emission quantum yields ($\Phi_{\text{em}}^{\text{max}}$, determined at [M $^{n+}$] = 0.1 M) are listed in Table I; the trends in $\Phi_{\text{em}}^{\text{max}}$ and K_a correspond, indicating that the effect of the cation on the MLCT emission increases as the stability of the crown complex increases (vide infra).

The cation-induced increase in Φ_{em} probably arises because the "crowned" cation decreases the donor ability of the crown nitrogen. This raises the energy of the LLCT state, and as a result, ΔG_{ic} becomes unfavorable and k_{ic} decreases. This model is supported by cyclic voltammetry on **1** as a function of [Ca $^{2+}$]. The height of the anodic (A/A $^{+}$) wave decreases significantly as [Ca $^{2+}$] increases, and no new waves appear for $E < +1.70 \text{ V}$, demonstrating that the coordinated cation increases the oxidation potential of the azacrown moiety.¹¹ By using +1.70 V as a lower limit for $E_{1/2}(\text{A/A}^+)$, a lower limit for ΔG_{ic} is obtained (+0.45 eV),²⁰ which supports the hypothesis that internal conversion is endoergic in the **1**...M $^{n+}$ complexes.

Although this model qualitatively accounts for the effect of cations on **1**, a more quantitative model is required to explain two experimental observations: (1) $\Phi_{\text{em}}^{\text{max}}$ and τ_{em} for the **1**...M $^{n+}$ complexes increase as K_a increases, and (2) $\Phi_{\text{em}}^{\text{max}}$ and τ_{em} for the **1**...M $^{n+}$ complexes are lower than for model **2**. Both of these observations are accounted for by the model presented in Scheme 1. Photoexcitation of **1**...M $^{n+}$ produces the MLCT state, which can decay via normal radiative and nonradiative pathways. However, this scheme also includes a nonradiative decay pathway involving rate-determining dissociation of the crowned cation (k_{off}), followed by rapid and irreversible formation of the LLCT state

Scheme 1



(k_{ic}). It is reasonable to expect that k_{off} will depend on the identity of the metal ion; thus, the addition of cation dissociation as a nonradiative decay pathway for the MLCT state affords an explanation for the cation-dependent variation of $\Phi_{\text{em}}^{\text{max}}$ and τ_{em} . The hypothesis that variation of $\Phi_{\text{em}}^{\text{max}}$ and τ_{em} arises from variation in the rate of a nonradiative process is supported by the observation of comparable radiative decay rates for the **1**...M $^{n+}$ complexes and **2** (k_r , Table I). Under the assumption that $k_{\text{ic}} \gg k_{\text{off}}[\text{M}^{n+}]$, the following expressions can be written for $\Phi_{\text{em}}^{\text{max}}$ and τ_{em} :

$$\Phi_{\text{em}}^{\text{max}} = k_r / (k_r + k_{\text{nr}} + k_{\text{off}}) \quad (2a)$$

$$\tau_{\text{em}} = 1 / (k_r + k_{\text{nr}} + k_{\text{off}}) \quad (2b)$$

It is clear from these expressions that $\Phi_{\text{em}}^{\text{max}}$ and τ_{em} will vary if k_{off} is cation-dependent. By using τ_{em} of **2** to provide an estimate for the "normal" MLCT state decay rate (e.g., $k_r + k_{\text{nr}}$), k_{off} can be estimated from τ_{em} for the **1**...M $^{n+}$ complexes.²² The values thus obtained are $1.3 \times 10^8 \text{ s}^{-1}$ (Na $^+$), $2.4 \times 10^7 \text{ s}^{-1}$ (Ba $^{2+}$), and $1.0 \times 10^7 \text{ s}^{-1}$ (Ca $^{2+}$). These off rates are in accord with rates determined by ultrasonic absorption.²³

This "dynamic" model is supported by the effect of protonation on the photophysical properties of **1**. The UV-visible absorption spectrum of **1**...H $^+$ is nearly identical with the absorption of model complex **2**. In addition, Φ_{em} and τ_{em} are substantially larger for the protonated complex (Table I). The significant feature is that Φ_{em} and τ_{em} for **1**...H $^+$ are quite similar to the values for model complex **2**. This coincidence suggests that when the rate of cation dissociation (in this case, deprotonation) is not competitive with the normal MLCT decay rate, then the photophysical properties of the MLCT chromophore in **1** and model complex **2** are very similar.

This work demonstrates a technique for development of a cation sensor based on a luminescent MLCT chromophore.²⁴ In addition, the study reveals that the sensitivity of complex **1** is limited by the kinetic instability of the crown-cation complexes, suggesting that the lability of the cation-ionophore complex must be decreased in order to optimize the cation-induced enhancement of the MLCT emission. Work in progress using multicyclic azacryptand ligands is directed toward this goal.²⁶

Acknowledgment. Acknowledgment is made to the donors of the Petroleum Research Fund, administered by the American Chemical Society, for support of this research.

(22) Under the assumptions that (a) k_r and k_{nr} are approximately the same for the **1**...M $^{n+}$ complexes and **2** and (b) $k_{\text{off}}[\text{M}^{n+}] \ll k_{\text{ic}}$, then k_{off} can be approximated by the expression $k_{\text{off}} \approx 1/\tau - 1/\tau_2$, where τ and τ_2 are the emission lifetimes of the **1**...M $^{n+}$ complexes and **2**, respectively.

(23) Liesegang, G. W.; Farrow, M. M.; Vazquez, F. A.; Purdie, N.; Eyring, E. M. *J. Am. Chem. Soc.* **1977**, *99*, 3240.

(24) Assuming that the detection limit (DL) is given by [cation] necessary to achieve $S/N \geq 3$ (ref 25), DL values using **1** with the alkali and alkaline earth cations in CH $_3$ CN solution are estimated to be Na $^+$, 0.007 M; Ba $^{2+}$, 0.001 M; Ca $^{2+}$, 0.0001 M. By using azacryptands (ref 26) to increase the kinetic and thermodynamic stability of the crown-cation complexes, the DL values very likely can be increased by several orders of magnitude in CH $_3$ CN. It is also possible that azacryptands will allow useful DL in aqueous solution.

(25) Ingle, J. D., Jr.; Crouch, S. R. *Spectrochemical Analysis*; Prentice Hall: Englewood Cliffs, NJ, 1988.

(26) Lehn, J.-M. *Angew. Chem., Int. Ed. Engl.* **1988**, *27*, 89.

(19) A similar CT band is observed in the free ligand.

(20) The driving force for internal conversion is estimated by $\Delta G_{\text{ic}} = E_{1/2}(\text{A/A}^+) - E_{1/2}(\text{bpy/bpy}^{\cdot-}) - E_{\text{MLCT}}$, where $E_{1/2}$ refers to the half-wave potentials of the redox processes (defined in text) and E_{MLCT} is the energy of the MLCT state. E_{MLCT} is estimated from computer fits of the emission spectra (ref 1b).

(21) Burgermeister, W.; Winkler-Oswatitsch, R. *Top. Curr. Chem.* **1977**, *69*, 91.